# Elevation Changes of Central Posterior Corneal Surface After Intracorneal Ring Segment Implantation in Keratoconus

*Esin Söğütlü, MD, PhD,* David P. Piñero, PhD,†‡ Anil Kubaloglu, MD,* Jorge L. Alio, MD, PhD,†§ and Yasin Cinar, MD**

**Purpose:** To compare changes that occur at the posterior corneal surface after the implantation of intracorneal ring segments (ICRSs) using either mechanical or femtosecond laser–assisted procedures and to correlate these changes with the visual outcome achieved.

**Methods:** Retrospective, nonrandomized, and interventional case series including 223 consecutive eyes of 186 patients with keratoconus ranging in age from 16 to 39 years that were implanted with ring segments (KeraRing; Mediphacos) at Kartal Training and Research Hospital, Istanbul, Turkey. Two groups were created according to the surgical technique used: mechanical group (168 eyes) and femtosecond group (55 eyes). Visual and refractive outcomes and corneal elevation changes were evaluated during a 24-month follow-up. Correlations between visual and posterior elevation changes were evaluated.

**Results:** The posterior corneal surface could not be analyzed with accuracy for diameters larger than the diameter of the ICRS implant. A statistically significant reduction of maximum elevation for both the corneal surfaces was observed at 1 month after the surgery ($P < 0.01$), with additional reductions at 3 and 6 months ($P \leq 0.03$). In addition, the posterior best-fit sphere was flattened significantly at 1 month after the surgery in both the groups, with additional flattening at 3 months ($P \leq 0.03$). No significant differences between groups in posterior corneal elevation parameters were found at any time point of the follow-up ($P \geq 0.14$). Moderate and significant correlations of the postoperative visual outcome with the change in posterior best-fit sphere were found only in the femtosecond group.

**Conclusions:** A central corneal flattening of the posterior corneal surface occurs after ring segment implantation in keratoconus.

**Key Words:** keratoconus, intracorneal ring segments, KeraRing, posterior corneal surface, Pentacam

(*Cornea* 2011;0:1–9)

Received for publication December 20, 2010; revision received May 1, 2011; accepted May 14, 2011.

From the *Kartal Training and Research Hospital, Istanbul, Turkey; †Keratoconus Unit, Vissum/Instituto Oftalmológico de Alicante, Alicante, Spain; ‡Departamento de Óptica, Farmacología y Anatomía, Universidad de Alicante, Alicante, Spain; and §Division of Ophthalmology, Universidad Miguel Hernández, Alicante, Spain.

Supported in part by a grant from the Spanish Ministry of Health, Instituto Carlos III, Red Temática de Investigación Cooperativa en Salud "Patología ocular del envejecimiento, calidad visual y calidad de vida", Subproyecto de Calidad Visual (RD07/0062).

The authors state that they have no financial or conflicts of interest to disclose.

Reprints: David P. Piñero, Avda de Denia s/n, Edificio Vissum, 03016 Alicante, Spain (e-mail: jlalio@vissum.com).



Keratoconus is a progressive, bilateral, and usually asymmetrical ectatic corneal disease, which is characterized by paraxial stromal thinning and weakening that leads to anterior corneal surface distortion.[1–8] This anterior corneal distortion induces an increase in regular and irregular astigmatism and therefore of both lower- and higher-order corneal aberrations.[1–8] The biomicroscopic findings in keratoconus, such as stromal thinning and posterior stress line, suggest that posterior corneal shape may be altered, possibly independent of that of the anterior surface. Tomidokoro et al[9] found that both anterior and posterior curvatures were affected in keratoconus and also in keratoconus suspect eyes. In these 2 groups of corneas, they found significantly larger values of spherical power, regular astigmatism, and higher-order irregularity in the posterior surface when compared with normal controls. Their results indicate that local protrusion occurs not only in the anterior corneal surface but also in the posterior corneal surface of keratoconic eyes. Therefore, it seems clear that manifestations of keratoconus also occur at the posterior corneal surface, even in early stages of the disease. The presence of a significant irregularity at the posterior corneal surface can have an influence on the retinal image quality, although the optical contribution of this surface is limited because it separates 2 media with refractive indices of close values.

Intracorneal ring segments (ICRSs) have been proposed and investigated as a surgical treatment option for keratoconus,[10–16] providing an interesting alternative aimed to delaying and prevent a corneal graft in patients with keratoconus.[13,14] This kind of surgical treatment has been proven to be effective in improving visual acuity, reducing the refractive error and mean keratometry.[13,14] It has been demonstrated that the addition of an ICRS at the corneal midperiphery induces a displacement of the local anterior surface forward at this area.[17] This modification in a normal cornea leads to a peripheral steepening and a flattening of the central portion of the anterior corneal surface due to the morphologic structure of corneal lamellae.[17] Similar behavior has been observed in keratoconic corneas,[11–16] although the response to the insertion of the implants seems to be more variable and complex. It should be considered that the stromal configuration is altered in the ectatic cornea, with a nonorthogonal lamellar architecture.[18] However, there are no studies reporting the type of changes occurring at the posterior corneal surface after ICRS implantation.

The aim of the current study was to analyze and compare changes that occur at the posterior corneal surface evaluated by means of a Scheimpflug imaging–based system

after ICRS implantation using either the mechanical procedures or the femtosecond laser–assisted procedures. Furthermore, the correlation among these corneal elevation changes and the visual outcome achieved were also investigated.

## MATERIALS AND METHODS

### Patients

This retrospective, nonrandomized, and interventional case series comprised 223 consecutive eyes of 186 patients with keratoconus that were implanted with ICRSs (KeraRing; Mediphacos, Belo Horizonte, Brazil) from August 2006 to August 2009 in Kartal Training and Research Hospital (Istanbul, Turkey). The mean patient age was 24.33 years (SD = 5.47; range, 16–39 years). All patients had a clear central cornea, and only patients dissatisfied with spectacle-corrected and contact lens–corrected vision were considered for ICRS implantation. Exclusion criteria were corneal thickness of 400 μm or less at the location where ICRS inserts were going to be placed (5-mm optical zone) in patients with a history of eye rubbing, acute hydrops, herpes keratitis, corneal dystrophies, diagnosed autoimmune disease, systemic connective tissue disease, and any other type of ocular active ocular disease. All patients were informed about the surgical procedure and its advantages and risks. During the process of consent for this surgery, consent was taken to later include clinical information in scientific studies. The informed consent obtained from patients was in accordance with the Declaration of Helsinki. All patients completed at least a 6-month follow-up. The mean follow-up time was 17.1 ± 7.5 months (range, 6–24 months).

### Surgical Procedure

All surgical procedures were performed under topical anesthesia by the same experienced surgeon (A.K.). The creation of corneal tunnels for ICRS implantation was performed by means of a mechanical dissection in 168 eyes (75.3%) and by means of femtosecond technology in 55 eyes (24.7%). For the creation of corneal tunnels by mechanical dissection, the Pentacam corneal thickness profile at the 5-mm corneal diameter zone was first analyzed to evaluate the viability of the surgery. Then, the pupil center was detected and marked as a reference point, and the ring location area was marked. The entry incision was made on the steepest corneal axis using a calibrated diamond blade. The tunnel depth was set at 70% of the thinnest corneal thickness. A suction ring (Moria, Inc) was then placed to minimize decentration, and the corneal tunnel was created by advancing within the corneal tissue a curved spatula in a counterclockwise and later in a clockwise direction. When the femtosecond technology was used, the corneal tunnel entry was made on the steepest corneal axis using the 15-kHz femtosecond laser (IntraLase; Advanced Medical Optics, Inc, Santa Ana, CA) and then the tunnels were created. In all cases, the tunnel depth was set at 70% of the thinnest corneal thickness. The inner to outer diameter of tunnels was set from 4.8 to 5.6 mm, the ring energy used for channel creation was 1.30 μJ, and the entry cut energy was 1.30 μJ. No particular inclusion/exclusion criteria were used in the current retrospective analysis for using mechanical or femtosecond techniques. Femtosecond technology was only applied when it was available at the hospital.

In all cases, KeraRing segments with an arc length of 160° (Mediphacos) were implanted using the manufacturer's forceps after tunnel creation. The segment thickness was determined based on the area of ectasia and spherical equivalent (SE) values according to the manufacturer's nomogram (Table 1). Lomefloxacin 0.3% (Okacin) and dexamethasone 0.1% (Dexa-Sin SE) eye drops were prescribed to be applied 2 times a day for 2 weeks after the surgery.

### Follow-up Examinations

A complete ophthalmic examination was performed in all eyes preoperatively and at 1 month and 3, 6, 18, and 24 months after ICRS implantation, including uncorrected distance visual acuity (UDVA), corrected distance visual acuity (CDVA), manifest subjective refraction, and corneal topographic analysis using a Scheimpflug photography-based system (mean keratometric reading in the 3-mm central zone and elevation data). UDVA and CDVA were measured in decimal Snellen and converted to the logarithm of the minimum angle of resolution for statistical analysis. Anterior and posterior corneal curvature and elevation measurements were obtained with the Scheimpflug camera system

**TABLE 1.** Nomogram for the Selection of the KeraRing Segment to Implant in Each Patient: Segment Distribution and Thickness According to the Area of Ectasia and SE Values*

| SE (D) | All Ectasia Is Limited to One Half of the Cornea | 75% of the Ectasia in One Half of the Cornea and 25% Situated in the Other Half | Two Thirds of the Ectatic Area in One Half of the Cornea and One Third in the Other Half | Ectasia Is Distributed Evenly in Both Corneal Halves |
|---|---|---|---|---|
| >−10 | 25/35 | 25/35 | 30/35 | 35/35 |
| −8 to −10 | 20/30 | 20/30 | 25/30 | 30/30 |
| −6 to −8 | 15/25 | 15/25 | 20/25 | 25/25 |
| −2 to −6 | 0/20 | 0/20 | 15/20 | 20/20 |
| <−2 | 0/15 | 0/15 | 15/15 | 15/15 |

*For defining the distribution of the ectasia, the cornea was divided into 2 halves using the steepest meridian as a reference. Nomogram notation: 25/35 = upper segment thickness/lower segment thickness (0.25/0.35 mm).

Pentacam HR (Oculus Optikgeräte, Wetzlar, Germany). With this system, a rotating Scheimpflug camera takes 100 images with 500 measurement points on the anterior and posterior corneal surfaces over a 180-degree rotation around the optical axes of the eye. The elevation data from these images are combined to form a 3-dimensional reconstruction of the corneal structure. In the current study, the high-resolution mode was used to obtain 50 images of each eye. It has been demonstrated that the Pentacam technology provides repeatable and reproducible pachymetric and geometrical measurements (anterior and posterior curvature, asphericity, elevation).[19–23] Specifically, Pentacam software version 6.02r10 was used in the current series (Fig. 1).

The best-fit sphere (BFS) for the posterior corneal surfaces in the central 4.5 mm was obtained in all cases. In addition, measurement of the maximum elevation for the anterior and posterior corneal surfaces was recorded in all cases at each visit [anterior maximum elevation (AME) and posterior maximum elevation (PME)]. This parameter was defined as the highest elevation value of the multiple readings in each quadrant of the numerical elevation map in a 4.5-mm zone. The reason for the selection of this area of analysis was the limitation observed in the reconstruction of the posterior corneal surface for larger diameters after ICRS implantation. Specifically, the software of the Pentacam system was not able to reconstruct the posterior corneal surface behind the location of the ring segments and then only the central area of the cornea could be analyzed with accuracy. Figure 1 shows a picture of such limitation (not continuous delimitation of the posterior corneal surface). All Scheimpflug pictures taken in the study with the Pentacam system were reviewed carefully to ensure that the central area of the posterior cornea was properly reconstructed and analyzed (complete and adequate tracing at this area). Elevation measurements derived from Scheimpflug images not showing an adequate tracing of the central portion of the posterior corneal surface were ruled out and not included in the analysis. It should be considered that the interest in studying the maximum elevation lay in knowing if the maximum difference with the mean curve fitting best to the corneal contour changed. This maximum elevation revealed how the cornea differed from a spherical curve, and it was expected to be largest when there were significant local variations of curvature, such as in keratoconus. For this reason, we did not use the same spherical curve for all cases as a reference when calculating the maximum elevation. The aim of the elevation data analysis was to evaluate if this maximum elevation decreased significantly and then the level of irregularity with respect to the best spherical fit to the corneal contour. Theoretically, maximum elevation for the anterior and posterior corneal surfaces should diminish after ICRS implantation because a corneal regularization is induced, which avoids the effect of the keratoconic corneal protrusion.

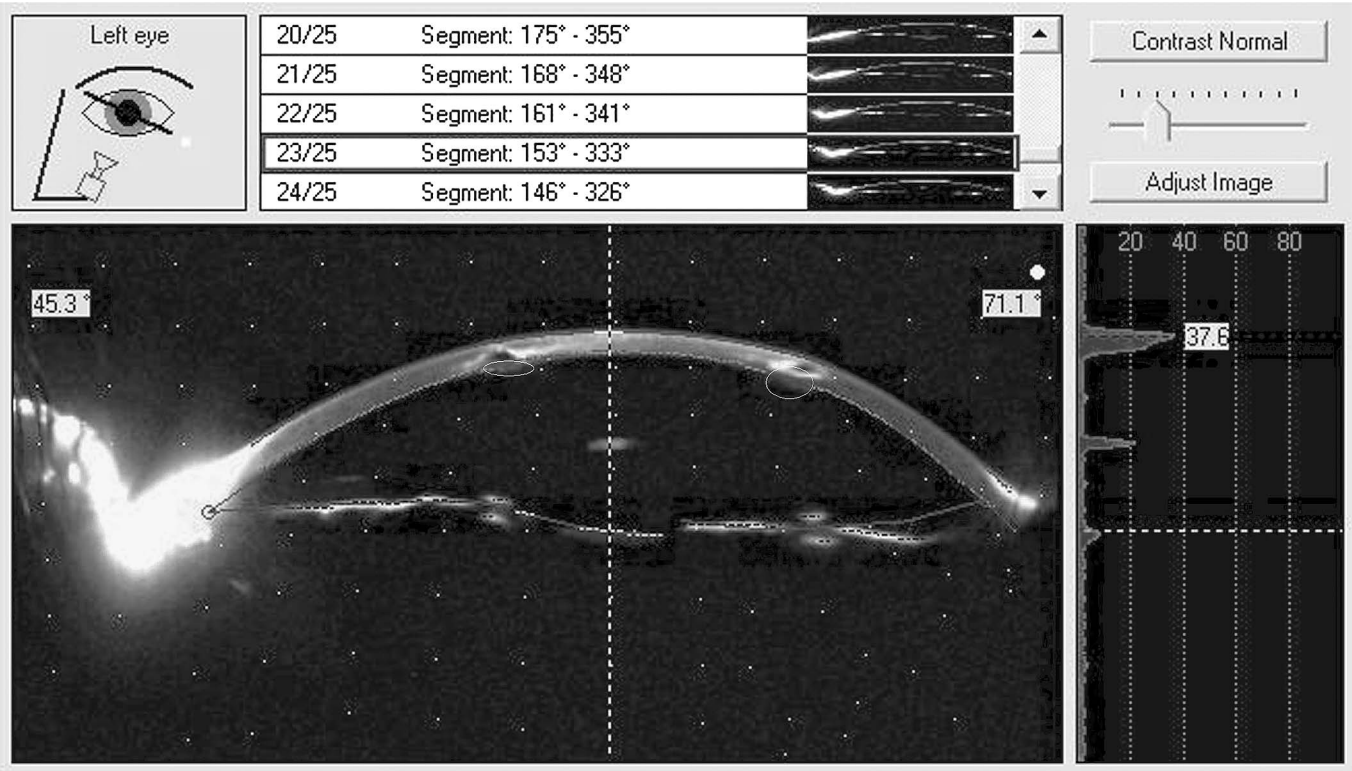


**FIGURE 1.** Example of a Scheimpflug scan obtained by means of the Pentacam system in 1 eye with keratoconus implanted with intracorneal ring segment from the sample of the current study. As shown, a limitation in the reconstruction of the posterior corneal surface behind the location of the ring segments is present (white circles). Specifically, the software of the Pentacam system is not able to reconstruct the posterior corneal surface behind the location of the ring segments and then only the central area of the cornea can be analyzed with accuracy.

## Statistical Analysis

SPSS statistics software package version 11.0 for Windows (SPSS, Chicago, IL) was used for statistical analysis. Normality of all data samples was first checked by means of the Kolmogorov–Smirnov test. When parametric analysis was possible, the Student *t* test for paired data was performed for all parameter comparisons between preoperative and postoperative examinations and the Student *t* test for unpaired data was used for evaluating differences among corneal tunnelization groups (mechanical vs. femtosecond). On the contrary, when parametric analysis was not possible, the Wilcoxon rank sum test was applied to assess the significance of differences between preoperative and postoperative data and the Mann–Whitney test was applied to evaluate differences among corneal tunnelization groups. The same level of significance ($P < 0.05$) was used in all cases. Correlation coefficients (Pearson or Spearman depending on whether a normality condition could be assumed) were used to assess the correlation between different variables.

# RESULTS

A total of 83 men (44.6%) and 103 women (55.4%) were included in this study. Only 37 cases were bilateral. The overall sample of eyes (223 eyes) was divided into 2 groups according to the surgical technique used for the creation of the channels where the ring segments were going to be implanted: eyes with ICRS implantation using the mechanical dissection (mechanical group, 168 eyes) and eyes with ICRS implantation using the femtosecond technology (femtosecond group, 55 eyes). As shown in Table 2, no significant differences were found preoperatively between these 2 groups in age, visual acuity, central pachymetry, and anterior and posterior corneal shape configuration (Mann–Whitney test, $P \geq 0.17$). Only the preoperative SE differed significantly between groups, with a trend to a more negative SE in the femtosecond group (Mann–Whitney test, $P = 0.01$). In addition, no significant differences were found in the surgical planning between groups (Mann–Whitney test, $P \geq 0.05$).

## Visual and Refractive Outcomes

In both the groups, a statistically significant improvement in UDVA (Wilcoxon test: mechanical, $P < 0.01$; femtosecond, $P < 0.01$) and CDVA (Wilcoxon test: mechanical, $P < 0.01$; femtosecond, $P < 0.01$) was found at 1 month after the surgery (Fig. 2). In addition, significant changes were also observed during the follow-up in the mechanical group: improvement in CDVA between postoperative months 1 and 3 (Wilcoxon test, $P = 0.01$) and improvement in UDVA between postoperative months 3 and 6 (Wilcoxon test, $P < 0.01$) (Fig. 2).

The significant improvement in UDVA was consistent with the significant reduction in the SE found in both the groups at 1 month after the surgery (Wilcoxon test: mechanical, $P < 0.01$; femtosecond, $P < 0.01$) (Fig. 3). Furthermore, in the mechanical group, an additional reduction of the SE was found between 1 and 3 months postoperatively (Wilcoxon test, $P = 0.04$).

When the comparison for visual acuity and refractive outcomes was performed between both the groups, no statistically significant differences were found in UDVA (Mann–Whitney test: 1 month, $P = 0.95$; 3 months, $P = 0.73$; 6 months, $P = 0.67$; 12 months, $P = 0.75$; 18 months, $P = 0.82$; and 24 months, $P = 0.49$) and CDVA (Mann–Whitney test: 1 month, $P = 0.74$; 3 months, $P = 0.81$; 6 months, $P = 0.98$; 12 months, $P = 0.99$; 18 months, $P = 0.46$; and 24 months, $P = 0.22$) during all follow-ups. Regarding the SE, the same trend was observed (Mann–Whitney test: 1 month, $P = 0.81$; 3 months, $P = 0.30$; 6 months, $P = 0.31$; 12 months, $P = 0.88$; 18 months, $P = 0.69$; and 24 months, $P = 0.47$) (Fig. 3).

## Corneal Topographic Changes

As expected, a significant central flattening of the anterior corneal surface was observed in both the groups at 1 month after the surgery (Wilcoxon test: mechanical, preoperative 50.94 ± 5.01 diopters (D), postoperative 47.78 ± 4.00 D, $P < 0.01$; femtosecond, preoperative 49.87 ± 4.30 D, postoperative 47.24 ± 4.51 D, $P < 0.01$) (Fig. 4). No significant changes were observed later in any of the groups (Wilcoxon test: mechanical, $P \geq 0.57$; femtosecond, $P \geq 0.21$). Regarding the maximum elevation, a statistically significant reduction of this parameter for both corneal surfaces was observed at 1 month after the surgery (Wilcoxon test: mechanical, $P < 0.01$; femtosecond, $P < 0.01$) (Fig. 5). Additional significant reductions were observed for both the groups between postoperative months 1 and 3 (Wilcoxon test:

**TABLE 2.** Preoperative Conditions of Patients Included in the 2 Groups of Eyes Analyzed in the Current Study

| Parameters | Mechanical Group (168 Eyes) | Femtosecond Group (55 Eyes) | *P* (Statistical Test) |
|---|---|---|---|
| Age, yr | 24.23 ± 5.40 (16 to 39) | 24.62 ± 5.73 (16 to 35) | 0.68 (Mann–Whitney) |
| Sex (M/F), % | 44.29/55.71 | 45.65/54.35 | 0.87 ($\chi^2$) |
| LogMAR UDVA | 1.13 ± 0.54 (0.15 to 3.00) | 1.15 ± 0.45 (0.00 to 2.00) | 0.42 (Mann–Whitney) |
| SE (D) | −4.46 ± 3.37) (−16.00 to +0.25) | −5.61 ± 3.41 (−18.25 to +1.00) | 0.01 (Mann–Whitney) |
| LogMAR CDVA | 0.68 ± 0.43 (0.00 to 2.00) | 0.61 ± 0.36 (0.00 to 1.70) | 0.56 (Mann–Whitney) |
| Mean anterior keratometry (D) | 50.94 ± 5.01 (40.35 to 68.80) | 49.87 ± 4.30 (43.15 to 62.15) | 0.17 (Mann–Whitney) |
| AME (μm) | 42.21 ± 15.38 (10 to 76) | 40.20 ± 14.59 (12 to 69) | 0.48 (Mann–Whitney) |
| PME (μm) | 53.86 ± 13.42 (18 to 89) | 52.09 ± 13.60 (21 to 79) | 0.43 (Mann–Whitney) |
| 4.5-mm PBFS (mm) | 5.98 ± 0.28 (5.39 to 6.87) | 6.01 ± 0.27 (5.67 to 6.65) | 0.55 (Mann–Whitney) |
| Central corneal thickness (μm) | 461.59 ± 61.92 (335 to 605) | 472.71 ± 36.50 (383 to 550) | 0.28 (Mann–Whitney) |

Values are represented as mean ± SD (range).
*$P$ values for the comparison between both the groups are shown for each parameter evaluated.
F, female; M, male; PBFS, posterior best-fit sphere.

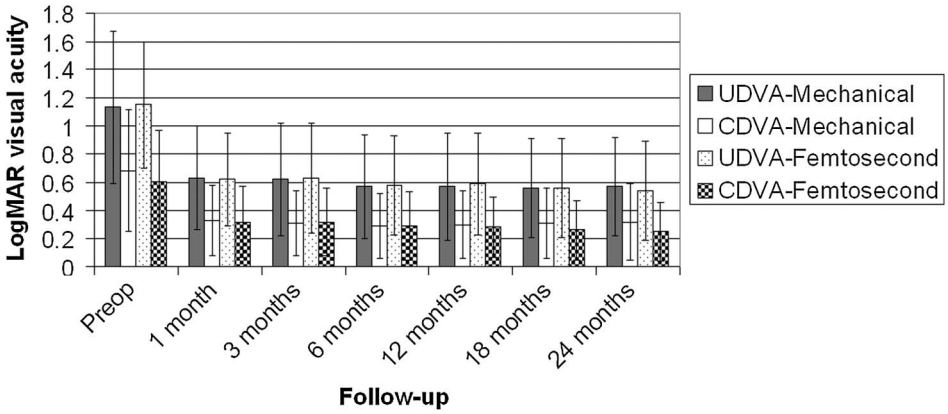


**FIGURE 2.** Changes in visual acuity during the follow-up in the mechanical and femtosecond groups (UDVA-mechanical, grey bars; UDVA-femtosecond, dotted bars; CDVA-mechanical, white bars; and CDVA-femtosecond, checked bars).

mechanical, $P < 0.01$; femtosecond, $P < 0.01$) and between months 3 and 6 (Wilcoxon test: mechanical, $P < 0.01$; femtosecond, $P \leq 0.03$). However, at 12 months after the surgery, a small but statistically significant increase of PME was observed for both the groups (Wilcoxon test: mechanical, $P < 0.01$; femtosecond, $P = 0.01$), with a significant posterior partial recovery of this reduction at 18 months (Wilcoxon test: mechanical, $P = 0.04$; femtosecond, $P < 0.01$). At 24 months, no significant changes in maximum corneal elevation were detected in any of the groups (Wilcoxon test: mechanical, $P = 0.38$; femtosecond, $P = 0.11$). When comparing the posterior maximum corneal elevation between groups, no significant differences were found at any time point of the follow-up (Mann–Whitney test: 1 month, $P = 0.41$; 3 months, $P = 0.20$; 6 months, $P = 0.37$; 12 months, $P = 0.83$; 18 months, $P = 0.71$; and 24 months, $P = 0.79$).

The posterior BFS for a 4.5-mm diameter increased significantly at 1 month after the surgery in both the groups (Wilcoxon test: mechanical, $P < 0.01$; femtosecond, $P < 0.01$) (Fig. 6). Additional increments of the posterior BFS were observed in both the groups between postoperative months 1 and 3 (Wilcoxon test: 4.5 mm, mechanical, $P < 0.01$; femtosecond, $P = 0.05$), in the mechanical group between postoperative months 18 and 24 (Wilcoxon test, $P = 0.02$), and in the femtosecond group between postoperative months 3 and 6 (Wilcoxon test, $P = 0.02$) (Fig. 6). No significant differences between groups were observed in the posterior BFS at any time point of the follow-up (Mann–Whitney test: 1 month, $P = 0.61$; 3 months, $P = 0.47$; 6 months, $P = 0.22$; 12 months, $P = 0.97$; 18 months, $P = 0.94$; and 24 months, $P = 0.36$).

In the mechanical group, very poor correlations were found between the change in the posterior BFS and the immediate postoperative visual and refractive outcomes (1 month: change in BFS-UDVA, $r = -0.07$ and $P = 0.38$; change in BFS-CDVA, $r = -0.01$ and $P = 0.95$; and change in BFS-SE, $r = 0.13$ and $P = 0.14$). Poor correlations were also found among the change in the posterior BFS and the late postoperative visual and refractive outcomes (24 months: change in BFS-UDVA, $r = 0.12$ and $P = 0.28$; change in BFS-CDVA, $r = 0.10$ and $P = 0.38$; change in BFS-SE, $r = 0.10$ and $P = 0.39$). Regarding the change in the maximum posterior corneal elevation, statistically significant correlations with vision and refraction were found during the follow-up, although they were weak (1 month: change in PME-UDVA, $r = -0.22$ and $P = 0.01$; change in PME-CDVA, $r = -0.28$ and $P < 0.01$; change in PME-SE, $r = 0.18$ and $P = 0.02$; 24 months: change in PME-UDVA, $r = -0.28$ and $P = 0.01$; change in PME-CDVA, $r = -0.29$ and $P = 0.01$; change in PME-SE, $r < 0.01$ and $P = 0.99$).

In the femtosecond group, poor and no significant correlations were found between the change in PME and in the immediate (1 month: change in PME-UDVA, $r = -0.06$ and $P = 0.68$; change in PME-CDVA, $r = -0.08$ and $P = 0.56$; change in PME-SE, $r = 0.10$ and $P = 0.54$) and late (24 months: change in PME-UDVA, $r = -0.26$ and $P = 0.27$; change in PME-CDVA, $r = -0.22$ and $P = 0.30$; change in PME-SE, $r = 0.08$ and $P = 0.75$) postoperative visual and refractive outcomes. Poor correlations were also found between the change in the posterior BFS and the visual and refractive outcomes but only in the initial postoperative period (1 month: change in BFS-UDVA, $r = 0.05$ and $P = 0.72$; change in BFS-CDVA, $r = -0.11$ and $P = 0.42$; change in BFS-SE, $r = 0.25$ and $P = 0.11$). At the end of the follow-up, the correlation between the visual outcomes and the change in the posterior BFS became statistically significant and stronger (24 months: change in BFS-UDVA, $r = -0.43$ and $P = 0.04$; change in BFS-CDVA, $r = -0.41$ and $P = 0.05$).

In addition, it should be also considered that a strong and statistically significant correlation was found between the change in the maximum corneal elevation value for both

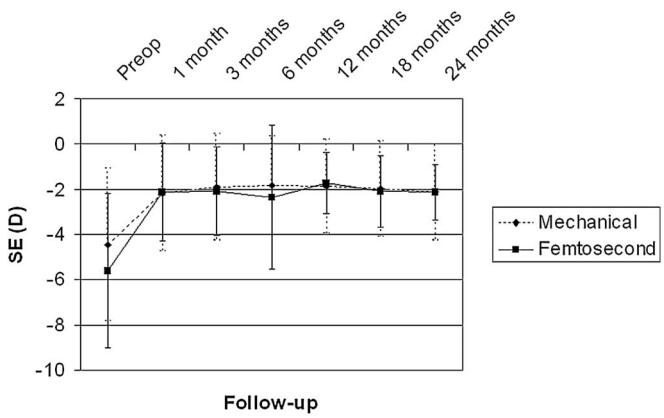


**FIGURE 3.** Changes in the SE during the follow-up in the mechanical (dotted line) and femtosecond (smooth line) groups.

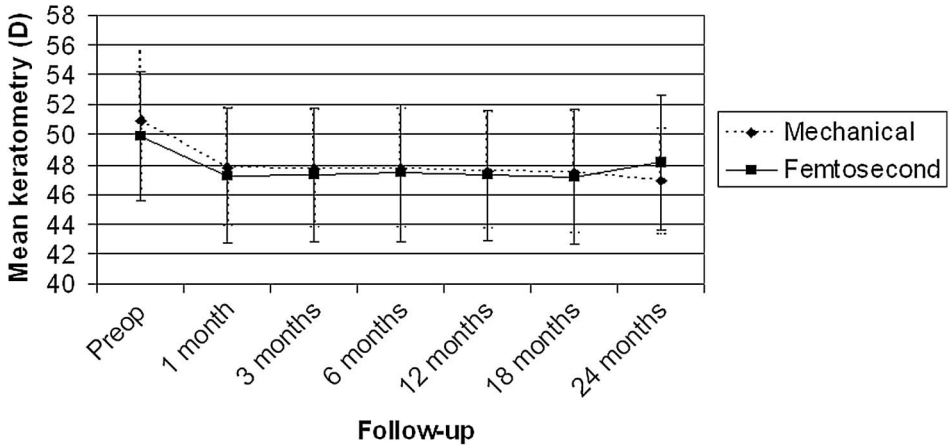


**FIGURE 4.** Changes in the anterior mean keratometry during the follow-up in the mechanical (dotted line) and femtosecond (smooth line) groups.

corneal surfaces in both the groups (mechanical group: $r = 0.61$ and $P < 0.01$; femtosecond group: $r = 0.73$ and $P < 0.01$).

## Correlation Among Anterior and Posterior Corneal Surfaces

Changes with surgery in the ratio of the anterior to the PME values were also analyzed in both mechanical and femtosecond groups. In both the groups, a progressive significant reduction of this ratio was observed during the postoperative follow-up (Wilcoxon test: preoperative to postoperative month 24, $P < 0.01$ for both the groups). In the mechanical group, the analyzed ratio changed from a mean preoperative value of 0.77 (range, 0.43–1.28) to a mean postoperative value of 0.56 (range, 0.35–1.58) at 24 months after the surgery. In the femtosecond group, the analyzed ratio changed from a mean preoperative value of 0.76 (range, 0.57–1.13) to a mean postoperative value of 0.56 (range, 0.36–0.73) at 24 months after the surgery.

## DISCUSSION

In the last few years, several authors have reported changes in the posterior corneal surface in early and advanced keratoconic eyes using different topographic systems.[5,9,24,25] Tomidokoro et al[9] reported by using the scanning-slit technology that a local protrusion occurred in both anterior and posterior surfaces of keratoconic corneas. Although the posterior corneal surface may be not optically as important as the anterior corneal surface,[26] its optical contribution can become relevant in keratoconus, especially when the curvature of this posterior surface is high (advanced keratoconus).[11] ICRSs have been proposed and investigated as an additive surgical procedure for keratoconus correction. Several studies have confirmed the efficacy and safety of ICRS implantation in reducing the refractive error and anterior corneal steepening using both mechanical and femtosecond laser–assisted tunnel creation.[11,16,27,28] ICRSs act as spacers between the bundles of corneal lamellae, shortening the central arc length and then inducing a flattening of the central portion of the anterior corneal surface.[17] However, the effect of ICRS

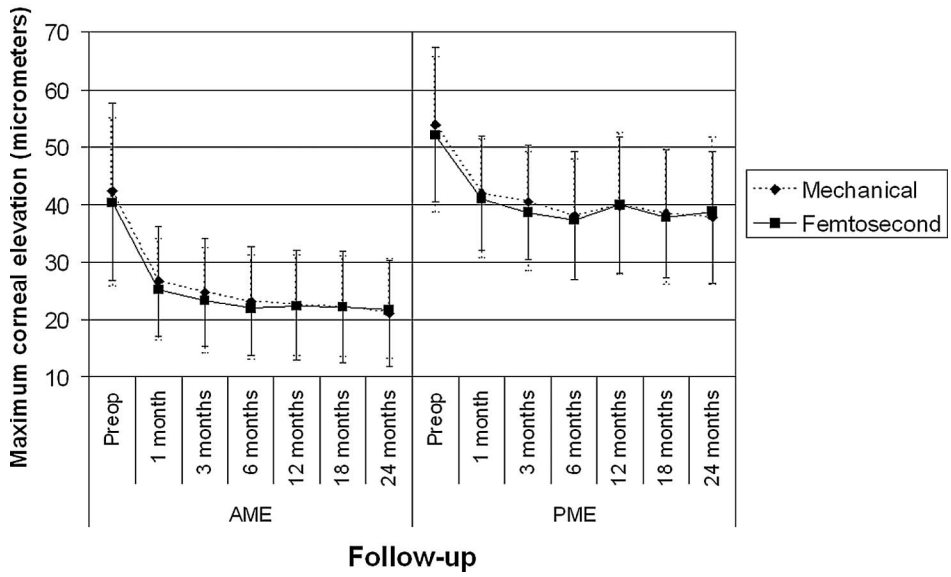


**FIGURE 5.** Changes in the AME PME during the follow-up in the mechanical (dotted lines) and femtosecond (smooth lines) groups.

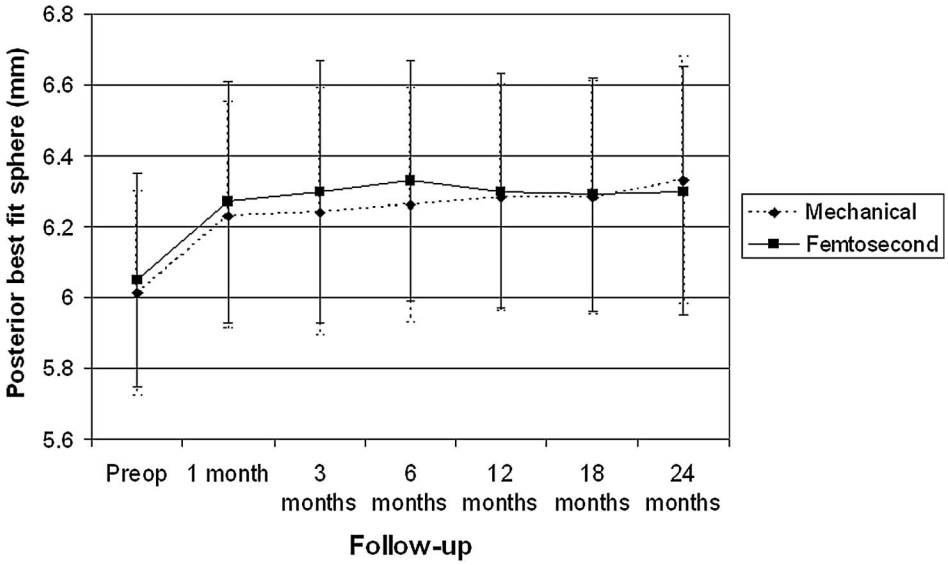


**FIGURE 6.** Changes in the posterior BFS for a 4.5-mm diameter during the follow-up in the mechanical (dotted line) and femtosecond (smooth line) groups.

implantation on the posterior corneal surface of keratoconus cornea still remains unknown. In the previous experience of our research group,[29] we found a reduction in the posterior corneal curvature after the implantation of Intacs in post–laser-assisted in situ keratomileusis ectatic corneas. We hypothesize that a flattening of the central area of the posterior corneal surface should be also observed in eyes with keratoconus implanted with ICRSs because the anterior and posterior corneal surfaces are parts from the same structure. Indeed, we have recently reported that changes in anterior and posterior corneal surfaces are correlated in keratoconus.[24] Therefore, the aim of the current study was to analyze and compare changes that occur in keratoconic corneas at the posterior corneal surface evaluated by means of a Scheimpflug imaging–based system after ICRS implantation using either the mechanical procedure or the femtosecond laser–assisted procedure. In addition, the correlations between posterior corneal surface changes and the postoperative visual outcome were investigated.

The Scheimpflug technology was used because it allows direct imaging of the posterior cornea. Specifically, the device used in the current study, the Pentacam system, has been proven to provide repeatable measurements of curvature, elevation, and asphericity for the posterior corneal surface in normal eyes.[19–23] However, we observed at the beginning of the study that the Pentacam was not capable of reconstructing the area of the posterior corneal surface behind the ring segments in all cases and then the system was unable to trace the complete contour of the posterior cornea (Fig. 1). To the best of our knowledge, this is the first time that this type of limitation of a Scheimpflug-based topography system is described. For this reason, only elevation changes of the central portion of the cornea (4.5 mm) were evaluated in the study because it was proven that the corneal contour reconstruction of the posterior corneal surface performed by the system at this area was correct.[19] The manufacturer should consider this limitation in future upgrades of the software because it seems to be only a limitation in the algorithm used for digital Scheimpflug image analysis.

The visual outcomes in the current study confirm the efficacy and safety of this surgical procedure. A statistically significant improvement in UDVA and CDVA was found after the surgery in both mechanical and femtosecond groups, which was consistent with previous findings of other authors.[11–14,27,28,30] Furthermore, a reduction of the SE was also observed in both the groups, which was consistent with the visual improvement. No significant differences were found between groups in these visual and refractive outcomes. This was consistent with a previous work of our research group comparing also the outcomes achieved with ICRS with the 2 different types of surgical implantation, mechanical and femtosecond guided.[11] The only discrepant finding with this previous article was the absence of statistical significance for the change in CDVA after the surgery in the mechanical group. A reason for this fact could be the lower percentage of advanced keratoconus included in the current sample of eyes. It should be remembered that the aberrometric control has been demonstrated to be significantly poorer in eyes with advanced corneal ectasia.[11] Another factor that could have accounted for this discrepancy was the inclusion in our previous work of patients operated on by several surgeons (multicenter study), and it should be remembered that the mechanical technique is highly dependent on the surgeon. This factor would have introduced a relevant variability in the outcomes because of the less interobserver repeatability of the procedure.[11]

Regarding the curvature changes in the anterior corneal surface, all findings were consistent with those previously reported.[11–16,27,28,30] A significant central flattening occurred after ICRS implantation, which was the reason for the reduction in the myopic SE. This flattening is due to the arc-shortening effect induced by the ICRSs because these implants act as spacer elements between the bundles of corneal lamellae at the mid periphery.[17] As could be expected, this change in

curvature was concordant with a significant change in maximum corneal elevation. In this study, we preferred to use elevation data for characterizing the change in corneal shape because it is the primary information derived from the Scheimpflug images obtained with the Pentacam system. Both AME and PME experienced a significant reduction at 1 month after the surgery, but also additional reductions occurred at 3 and 6 months. A consideration is that maximum elevation parameters can be considered as indirect estimators of the level of corneal irregularity (maximum difference with the mean curve fitting best to the corneal contour changed). We believe that the greatest part of the flattening effect occurs during the initial postoperative period according to the keratometric outcomes obtained, and, possibly, the increases in maximum elevation occurring later are the consequence of the regularization of the anterior and posterior corneal contour. This could explain the presence of visual improvements at intermediate periods during the follow-up. Indeed, our research group found nonimmediate corneal aberrometric changes after ICRS implantation in keratoconus.[11,27]

As commented, a significant reduction of the posterior corneal maximum elevation after the surgery was observed, but also a significant increase in the posterior BFS. These findings are logical because if the radius of curvature of a surface increases, the surface is flattened. The increase in posterior BFS after ICRS was not immediate. Changes in this parameter were detected even 3 months after the surgery in both the groups, and this reveals the progressive modeling of the corneal contour. However, in the mechanical group, a significant increase in posterior BFS was observed at the end of the follow-up. This suggests the presence of late biomechanical changes inducing posterior corneal contour modifications in eyes implanted with ICRS using this technique. This may be due to several factors, such as biomechanical keratoconic changes or the stabilization of the tunnelization performed manually. In any case, this slight late modification in the mechanical group did not result in a significant difference in the postoperative outcome obtained with the mechanical and femtosecond-guided techniques at the end of the follow-up. Regarding the changes induced in maximum posterior corneal elevation, they seemed to vary with time. At 12 months after the surgery, a small increase in PME was detected, with a partial but significant recovery at 18 months. This reveals the presence of changes in posterior corneal regularity 1 year after ICRS implantation because the BFS did not change significantly during this period. Therefore, corneal changes still occurred despite the implantation of the ring segments. It should be remembered that the ICRSs are able to model the cornea but not to stop the progression of the ectatic process.[11,31] These late changes in posterior corneal contour could be the result of keratoconic biomechanical changes. In any case, this is something that should be evaluated and studied more comprehensively in future studies. Furthermore, no significant differences between groups in any posterior corneal elevation changes during the follow-up were detected, which implies that the same central flattening effect is achieved with both types of surgical techniques. Another curious finding was the similar trend observed in the variation of the ratio of the AME to the PME in both mechanical and femtosecond groups. The ratio decreased in both the groups, which implied a larger flattening effect in the anterior corneal surface rather than in the posterior corneal surface. This seems logical because the main objective of the ICRS was to modify the anterior corneal shape, which is the optical surface of the eye with the major contribution to the total ocular refractive power.

As previously commented, correlations between posterior corneal changes and the achieved visual outcome were studied. No statistically significant correlations of the change in the posterior BFS and the visual acuity outcomes were obtained in the mechanical group. However, a limited inverse and statistically significant correlation was found between the late postoperative visual outcome and the change in posterior BFS in the femtosecond group. Specifically, as more significant posterior flattening was induced, the better the visual outcome was. Therefore, the flattening effect generated on the posterior cornea by the ICRS implanted using the femtosecond technology may have an influence on the visual outcome, with a potential clinical impact that can be perceived in some cases by the patient. Possibly, a less predictable and regular flattening effect is induced with the mechanical dissection in the posterior corneal surface, which may limit the potential visual benefit of the posterior corneal change. It has been demonstrated that the mechanical tunnelization for ICRS implantation is a more variable procedure depending on the surgeon's skills, with less control of corneal aberrations from the anterior surface.[11] In the mechanical group, significant negative correlations were found among the change in PME and the postoperative visual outcome, but they were extremely weak. Future studies and simulations should be performed to optimize the nomograms, considering the potential influence of the posterior corneal changes after ICRS implantation on the final visual outcomes. A mathematical modelization of the global change of the corneal structure with these implants would be desirable.

In summary, posterior corneal changes also occur in keratoconic corneas after ICRS implantation. Both the corneal surfaces are flattened in the central area by the effect of the implantation of the ring segments in the corneal mid periphery. This effect is equivalent using the 2 types of surgical procedures for the creation of the corneal tunnels for ICRS implantation, the mechanical dissection, and the femtosecond-guided tunnelization. However, this flattening effect has a positive effect on the visual outcomes only in those eyes operated on with the femtosecond–guided technique. The evaluation of the posterior corneal curvature after ICRS implantation in keratoconic eyes is also a useful tool for having a complete characterization of the ring segment effect. Future studies are necessary to evaluate the changes in posterior corneal aberrations with both types of surgical techniques for ICRS implantation. Posterior corneal changes should be also evaluated with other types of ICRS, such as Intacs. Furthermore, upgrades of the software of the Pentacam system allowing a more precise digital analysis and reconstruction of the posterior corneal surface are necessary. Thus, this specific Scheimpflug-based system will be able to be

perform a complete characterization of the posterior corneal contour after ICRS implantation.

## REFERENCES


1. Shirayama-Suzuki M, Amano S, Honda N, et al. Longitudinal analysis of corneal topography in suspected keratoconus. *Br J Ophthalmol*. 2009;93: 815–819.
2. Reeves SW, Ellwein LB, Kim T, et al. Keratoconus in the Medicare population. *Cornea*. 2009;28:40–42.
3. Li Y, Meisler DM, Tang M, et al. Keratoconus diagnosis with optical coherence tomography pachymetry mapping. *Ophthalmology*. 2008;115: 2159–2166.
4. Belin MW, Khachikian SS. Keratoconus: it is hard to define, but… *Am J Ophthalmol*. 2007;143:500–503.
5. McMahon TT, Szczotka-Flynn L, Barr JT, et al. CLEK Study Group. A new method for grading the severity of keratoconus: the Keratoconus Severity Score (KSS). *Cornea*. 2006;25:794–800.
6. Rabinowitz YS. Keratoconus. *Surv Ophthalmol*. 1998;42:297–319.
7. Rabinowitz YS, McDonnell PJ. Computer-assisted corneal topography in keratoconus. *Refract Corneal Surg*. 1989;5:400–408.
8. McGhee CN. 2008 Sir Norman McAlister Gregg Lecture: 150 years of practical observations on the conical cornea—what have we learned? *Clin Experiment Ophthalmol*. 2009;37:160–176.
9. Tomidokoro A, Oshika T, Amano S, et al. Changes in anterior and posterior corneal curvatures in keratoconus. *Ophthalmology*. 2000;107: 1328–1332.
10. Piñero DP, Alio JL, Teus MA, et al. Modeling the intracorneal ring segment effect in keratoconus using refractive, keratometric and corneal aberrometric data. *Invest Ophthalmol Vis Sci*. 2010;51:5583–5591.
11. Piñero DP, Alio JL, Kady BE, et al. Refractive and aberrometric outcomes of intracorneal ring segments for keratoconus: mechanical versus femtosecond-assisted procedures. *Ophthalmology*. 2009;116: 1675–1687.
12. Shabayek MH, Alió JL. Intrastromal corneal ring segment implantation by femtosecond laser for keratoconus correction. *Ophthalmology*. 2007; 114:1643–1652.
13. Kymionis GD, Siganos CS, Tsiklis NS, et al. Long-term follow-up of Intacs in keratoconus. *Am J Ophthalmol*. 2007;143:236–244.
14. Alió JL, Shabayek MH, Artola A. Intracorneal ring segments for keratoconus correction: long-term follow-up. *J Cataract Refract Surg*. 2006; 32:978–985.
15. Colin J, Cochener B, Savary G, et al. INTACS inserts for treating keratoconus: one-year results. *Ophthalmology*. 2001;108:1409–1414.
16. Colin J, Cochener B, Savary G, et al. Correcting keratoconus with intracorneal rings. *J Cataract Refract Surg*. 2000;26:1117–1122.
17. Patel S, Marshall J, Fitzke FW III. Model for deriving the optical performance of the myopic eye corrected with an intracorneal ring. *J Refract Surg*. 1995;11:248–252.
18. Meek KM, Tuft SJ, Huang Y, et al. Changes in collagen orientation and distribution in keratoconus corneas. *Invest Ophthalmol Vis Sci*. 2005;46: 1948–1956.
19. Piñero DP, Saenz González C, Alió JL. Intraobserver and interobserver repeatability of curvature and aberrometric measurements of the posterior corneal surface in normal eyes using Scheimpflug photography. *J Cataract Refract Surg*. 2009;35:113–120.
20. Shankar H, Taranath D, Santhirathelagan CT, et al. Anterior segment biometry with the Pentacam: comprehensive assessment of repeatability of automated measurements. *J Cataract Refract Surg*. 2008;34:103–113.
21. Chen D, Lam AK. Reliability and repeatability of the Pentacam on corneal curvatures. *Clin Exp Optom*. 2009;92:110–118.
22. Chen D, Lam AK. Intrasession and intersession repeatability of the Pentacam system on posterior corneal assessment in the normal human eye. *J Cataract Refract Surg*. 2007;33:448–454.
23. Kawamorita T, Uozato H, Kamiya K, et al. Repeatability, reproducibility, and agreement characteristics of rotating Scheimpflug photography and scanning-slit corneal topography for corneal power measurement. *J Cataract Refract Surg*. 2009;35:127–133.
24. Piñero DP, Alió JL, Alesón A, et al. Corneal volume, pachymetry, and correlation of anterior and posterior corneal shape in subclinical and different stages of clinical keratoconus. *J Cataract Refract Surg*. 2010; 36:814–825.
25. Schlegel Z, Hoang-Xuan T, Gatinel D. Comparison of and correlation between anterior and posterior corneal elevation maps in normal eyes and keratoconus-suspect eyes. *J Cataract Refract Surg*. 2008;34:789–795.
26. Turner T. What corneal topography can tell you about corneal shape. In: MacRae S, Krueger R, Applegate RA, eds. *Customized Corneal Ablation: The Quest for Supervision*. Thorofare, NJ: Slack Inc; 2001:221–227.
27. Piñero DP, Alió JL, El Kady B, et al. Corneal aberrometric and refractive performance of 2 intrastromal corneal ring segment models in early and moderate ectatic disease. *J Cataract Refract Surg*. 2010;36:102–109.
28. Alió JL, Shabayek MH, Belda JI, et al. Analysis of results related to good and bad outcomes of Intacs implantation for keratoconus correction. *J Cataract Refract Surg*. 2006;32:756–761.
29. Alió J, Salem T, Artola A, et al. Intracorneal rings to correct corneal ectasia after laser in situ keratomileusis. *J Cataract Refract Surg*. 2002; 28:1568–1574.
30. Ertan A, Kamburoglu G, Bahadir M. Intacs insertion with the femtosecond laser for the management of keratoconus: one year results. *J Cataract Refract Surg*. 2006;32:2039–2042.
31. Piñero DP, Alio JL, Barraquer RI, et al. Corneal biomechanical changes following intracorneal ring segment implantation in keratoconus. *Cornea*. In press.